Article

Applying Chemical and Statistical Analysis Methods to Evaluate Water and Stream Sediments around the Coal Mine Area in Dazhu, China

Dongping Deng [1,2], Yong Wu [1,2,*], Bangzheng Ren [3] and Heng Yin [1,2,4]

[1] College of Environment and Civil Engineering, Chengdu University of Technology, Chengdu 610059, China
[2] State Key Laboratory of Geohazard Prevention and Geoenvironment Protection, Chengdu 610059, China
[3] Institute of Ecology, China West Normal University, Nanchong 637009, China
[4] Sichuan Academy of Safety Science and Technology, Chengdu 610045, China
* Correspondence: ywu@cdut.edu.cn

Abstract: In this study, groundwater, stream water, and stream sediment samples were collected from a coal mine area in Dazhu, Southwestern China, and hydrogeochemical, multivariate, and X-ray analyses were conducted to examine the effects of coal mine pollution. The groundwater and stream samples were slightly acidic to alkaline (6.7 to 8.2). Typically, the water samples were dominated by Ca^{2+} + Mg^{2+}–HCO_3^- and Ca^{2+} + Mg^{2+}–Cl^-. SO_4^{2-} originates from gypsum dissolution and pyrite oxidation, and Ca^{2+} and Mg^{2+} may be related to the dissolution of carbonate. According to the Chinese standard and World Health Organization guidelines, the water in the coal mine area is of good quality in terms of its physical and chemical properties, except for the concentration of Mn and Fe, with values of 1925.14 μg/L and 12,872.88 μg/L, respectively. A principal component analysis revealed two groups in which the concentration of metals and metalloids in stream sediments are affected by the coal mine drainage. The Mn and Fe average concentration in the downstream Kongjiagou drain sediment samples was 2035.1 ppm and 6%, respectively. These values were higher than the average Mn and Fe concentration in Xiaojiagou at 453.1 ppm and 2.9%, respectively. Both the Mn and Fe concentration were higher than the background values (640 ppm and 4.4%).

Keywords: water; stream sediment; hydrochemistry; geochemistry; statistical analysis

1. Introduction

Chinese coal is one of the main sources of coal in the world, accounting for approximately 76% of the primary energy consumption in China, and it is predicted to remain the primary energy source in China in the long term [1].

Significant research has been conducted worldwide on the distribution characteristics and elemental sources of the coal and coal-bearing strata, as well as their effects on the environment. In Greece, the concentrations of As, Hg, Pb, and Sb in rocks and sediments of the Oropos–Kalamos basin were found to be significantly higher than the world average [2]. The mean values for As, Cr, and Hg in lignite coal in Thailand were found to be highly elevated compared to world coal values [3], and the coal seams were high in toxic and harmful elements, such as Cd, Cr, Cu, Ni, Mn, and Zn [4].

During mining, coal is continuously drained onto roads, in which oxygen enters the underground environment and oxidizes the pyrite in the coal, forming sulfate or even sulfuric acid after oxidation. These reactions generate acidic wastewater, which is usually referred to as acid mine drainage (AMD) [5]. AMD reacts with carbonate and silicate minerals in aquifers that are often rich in sulfuric acid and heavy metals [6]. In Australia, the Old Tailings Dam was found to generate AMD with a pH as low as 2.3–3.7 [7]. Furthermore, AMD containing high concentrations of Cd, Cr, Cu, and Fe in a coal mining area in India exceeds the desirable limits [8]. With the discharge of AMD, these elements

pollute surface water, stream sediment, and soil downstream from the outfall, which can seriously affect the quality of life and productivity of residents in the mining area. Moreover, AMD pollutes groundwater in other aquifers through cracks generated by coal mining [9].

In the 1990s, thousands of coal mines operated in China, most of which were small and distributed in the shallow areas of larger state-owned coal mines. By the end of 2016, the number of coal mines had plummeted to less than 8000, and more than 90,000 coal mines had closed in the previous 20 years [10]. With the closure of these coal mines, groundwater continuously pours into the closed mining area, resulting in a reduced groundwater environment that ceases pyrite oxidation. High concentrations of two opposing anions (SO_4^{2-} and HCO_3^{-}) in the Razi mine waters were evidence of the AMD generation and neutralization processes [11].

In Southwest China, particularly in the Sichuan Basin, most coal is mined in the Xujiahe Triassic Formation. The stratum of this area is clastic rock interlayer fissure water with high water inflow (100–500 t/d). Due to coal accumulation, coal and its strata in the sedimentary environment are enriched in heavy metals. Heavy metals migrate into the water and stream sediment during mining. These water and stream sediments affected by mining activities are widely distributed, resulting in a more representative analysis compared to that of a smaller distribution. Thus, studying the water and stream sediments from this study area can support water resource management, water quality evaluation, and water and stream sediment restoration.

In this study, the main objectives were (1) to analyze the physicochemical and chemical properties of the groundwater and stream flowing downstream from the coal mine drainage, (2) to assess the water and stream sediment quality based on the guidelines provided by the Chinese standard and World Health Organization [12], (3) to statistically analyze the correlations between the ions in the samples and determine the main contributing factors, and (4) to identify the correlations between coal mine drainage and stream sediments that affect the release and migration of pollutants into the study area.

2. Study Area

This study was conducted approximately 15 km northeast of Dazhu County, Dazhou City, Southwest Sichuan Province, China, which is under the administration of the Xinsheng Township of Dazhu County (Figure 1), and in the eastern Sichuan fold belt of the Neocathaysian Sichuan subsidence belt. It is composed of a series of anticlines and synclines, where the anticline is narrow, long, and compact, whereas the syncline is open and gentle, is arranged in an echelon, and has a northeast–southwest axial distribution. The natural watershed is composed of sandstone of the Xujiahe Triassic Formation, with high and low terrain to the west and east, respectively. As it is divided by the east–west transverse valley, the formed "V"-shaped valley is densely distributed in the whole area.

The study area has a subtropical monsoonal climate with four distinct seasons, including a warm, humid climate; heavy rainfall in the summer; and rain and fog in the winter, with an average frost-free period of 347 d. The annual average temperature is 18 °C, with extreme temperature values of −4.0 and 40.2 °C. The average and extreme annual precipitation values are approximately 1245.7 mm, and 840.9 and 1495.9 mm, respectively, where the precipitation from May to September accounts for 60% of that in the entire year. Abundant annual precipitation provides sufficient water supply for groundwater and stream formation.

The exposed strata in the study area include the Xujiahe Triassic Formation (T_3xj), Zhenzhuchong Jurassic Formation (J_1zh), Ziliujing Jurassic Formation ($J_{1-2}z$), and Xintiangou Jurassic Formation (J_2x) (Figure 1) [13]. The Xujiahe Formation is a coal-bearing stratum in an area with a continental sedimentary environment composed of dark grey mudstone, shale, fine sandstone, siltstone, and coal seam [14]. The Zhenzhuchong Formation is mainly composed of gray, greenish gray, and silty mudstone, with a small amount of purplish red mudstone in the upper part, several coal seams in the lower part, and a small amount of chert gravel at the bottom. The type of groundwater in both T_3xj and J_1zh is clastic rock

interlayer fissure water, where the water inflow of a single well is 100–500 t/d and the mineralization degree is less than 0.5 g/L. The Ziliujing Formation is mainly composed of grey to dark grey mudstone with a thin layer of argillaceous siltstone, which is rich in lamellibranchia fossils. The groundwater type is fissure karst water with suitable yield. The spring flow is 0.1–10 L/s, and the mineralization degree is 0.1–0.4 g/L. Finally, the Xintiangou Formation is composed of mudstone, silty mudstone, and fine sandstone, where sandstone is the aquifer and mudstone the relative aquifuge. The groundwater type is red bed confined water, in which the depth of the water-bearing part is approximately 30–150 m, and the water inflow of a single well is 100–500 t/d, with a mineralization degree of less than 0.5 g/L [15].
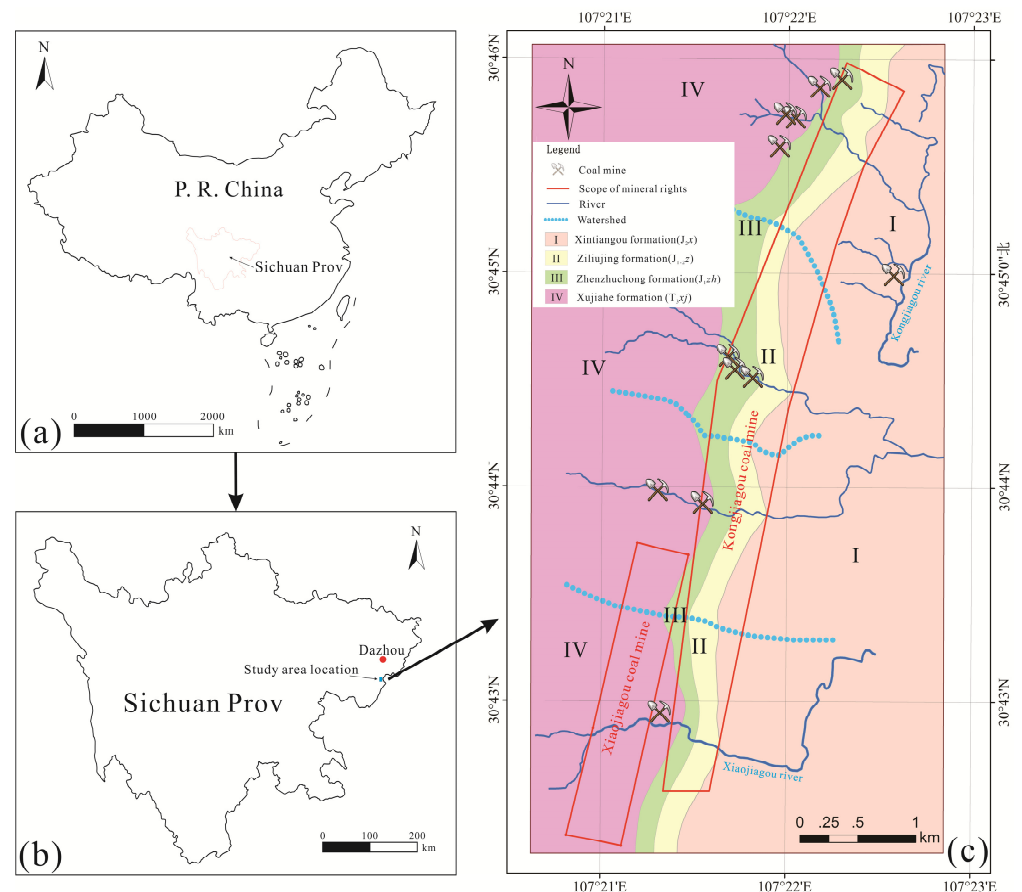

Figure 1. (**a**) The Sichuan Province in China, (**b**) location of study area in Sichuan Province, (**c**) geological and hydrogeological map of study area.

Since the 1960s, more than 10 coal mines have been operating in the chosen study area (Figure 1). Except for the Kongjiagou coal mine, which is still being mined, the other coal mines closed between 1990 and 2010 because of pollution and economic changes. A comprehensive development method for inclined shafts and adits is adopted at the Kongjiagou coal mine. An inclined shaft is used for air intake and the transportation of coal, gangue, materials, and equipment in the mine. An adit is used for auxiliary air intake, drainage, and pedestrians.

Once an abandoned coal mine ceases drainage, the groundwater level in the mine gradually rises and stabilizes with recharging by groundwater or surface water, forming a large water body [16]. Finally, the coal mine drainage flows out from the pithead as the mine water continues to fill. Local residents connect pipes to such pitheads for drinking or irrigation water (Figure 2a,b).

All coal mines in the study area are underground, and the coal seam is located in the Xujiahe Formation. Minerals such as quartz, feldspar, muscovite, pyrite, and filling

can be observed in the strata of the Xujiahe Formation. The output of these coal mines is mainly bright coal, followed by dark coal. Bright coal is strongly shiny with sandwich coal, dark coal, and a thin charcoal layer. Dark coal is shiny-light with a small amount of specular coal and silk charcoal. The average moisture content in the raw coal is less than 0.9%, the average yield of volatile matter (V_{daf}) is 29.04–33.36%, and the CO_2 content is less than 2% [17].

Figure 2. The study area: (**a**) coal mine drainage for agriculture, (**b**) pipes at the pithead, (**c**) drain of Xiaojiagou coal mine, (**d**) drain of Kongjiagou coal mine.

3. Materials and Methods

3.1. Data Collection and Sample Analysis

Mine drainage was found at the pitheads of five abandoned mines in the study area; therefore, five groundwater samples (P1–P5) were collected from the pitheads of these abandoned mines. Two groundwater samples (P7 and P8) were collected from the pitheads of the Xiaojiagou coal mine and Kongjiagou coal mine discharge downstream (Figure 2c,d). Eight stream water samples (P6, P9–P15) were collected at 0, 100, 500, and 1000 m from the mine drain. All samples, including groundwater samples and stream water samples, were collected once in both April 2020 (dry season in spring) and October 2020 (wet season in autumn), with a total of 30 samples. Seven stream sediment samples (S1–S7) and water samples (P9–P15) were collected simultaneously. All the sample locations, as shown in Figure 3, were recorded using the Global Positioning System.

The groundwater samples were collected 1–2 m below the well, and the stream water samples were collected 20 cm below the surface of the water. Each water sample was collected in two sealed, high-density polyethylene bottles, one of which was acidified with nitric acid to test for cations and trace elements. All water samples were stored at 5 °C and immediately transported to the laboratory for further analysis. Physicochemical parameters,

such as pH, Eh, dissolved oxygen, electrical conductivity (EC), and total dissolved solids (TDS), were measured in the field using a water-monitoring instrument (Aquaread AP-800, Broadstairs, UK). Major anions (Cl^-, SO_4^{2-}) were measured using ion chromatography with a 761 Compact IC Model (Metrohm AG, Herisau, Switzerland), and HCO_3^- was measured by titration. The detection limits of Cl^-, SO_4^{2-}, and HCO_3^- were 0.007 mg/L, 0.018 mg/L, and 2.5 mg/L, respectively. Water Quality-Determination of Inorganic Anions (HJ 84-2016) and Certified Reference Materials (201849 and 201935) were used to ensure the accuracy of Cl^-, and SO_4^{2-} concentrations. The major cations (K^+, Na^{2+}, Ca^{2+}, and Mg^{2+}) were analyzed using inductively coupled plasma atomic emission spectrometry (ICP-AES) (iCAP 7400, Thermo Fisher Scientific, Waltham, MA, USA), and the trace elements of Li, B, Al, Ti, Mn, Fe, Ni, Zn, Mo, and Ba were analyzed using inductively coupled plasma mass spectrometry (ICP-MS) (Agilent 7700, Agilent Scientific Instruments, Palo Alto, CA, USA). The ionic balance in all the analytical data was found to be within a limit of less than (±5%) by using geochemical speciation software (PHREEQC), which also could be used in thermodynamic calculation of the saturation indices.
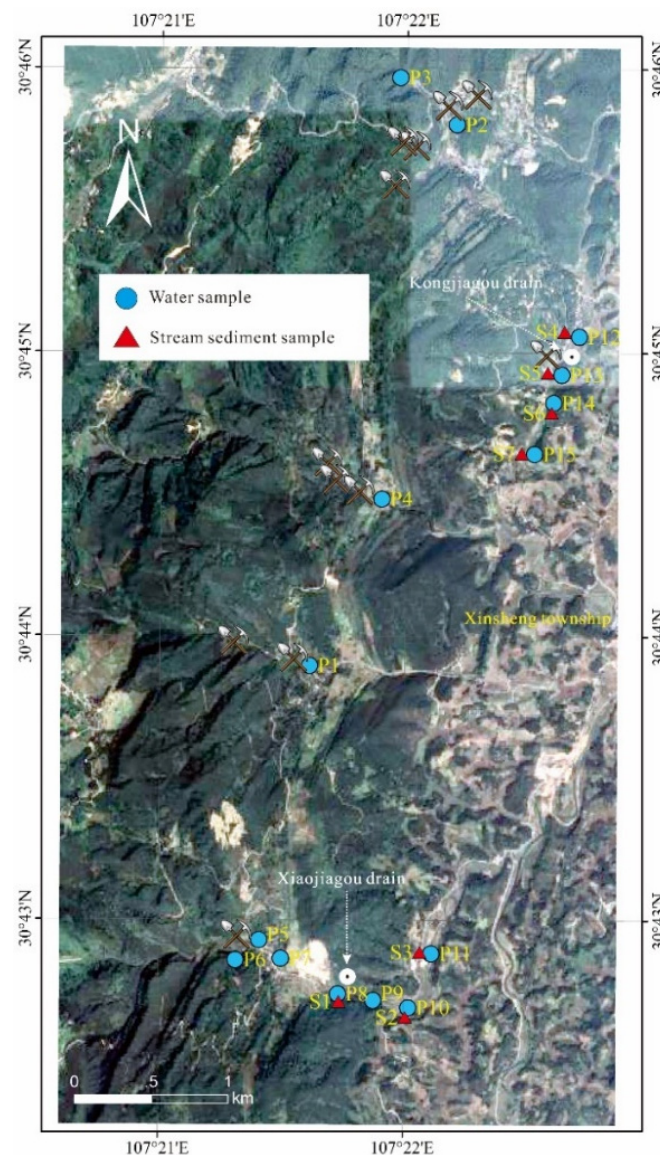

Figure 3. Distribution of samples in the study area.

Stream sediment samples were collected downstream of the mine drainage outlet at a depth of 10–20 cm (Figure 3), packed in black polyethylene bags, and transported to

the laboratory. After being air-dried, each sample was ground to <74 μm for the chemical analysis. The samples were digested using the method described in (DZ/T 0279-2016). ICP-MS and ICP-AES were used to determine the concentrations of 15 elements, including major oxides and trace elements such as Fe_2O_3, Al_2O_3, Mn, Cr, Cu, Pb, and Zn. The detection limits of all oxides were less than 0.01% and those of trace elements were less than 0.2 ppm. In addition, the standard sample (GBW07385: GSS-29) was analyzed as duplicates to ensure data reliability.

All tests were conducted at the Chengdu Comprehensive Rock and Mineral Testing Center of the Sichuan Provincial Bureau of Geology and Mineral Exploration and Development. To estimate the pollution levels of the groundwater and stream sediment in the study area, the guidelines for drinking water quality [12] and the Chinese standards for water and soil contamination were adhered to and referred to in this study.

Mineralogical characterization of the samples (S1 and S4) was performed by X-ray diffraction (XRD) using a Rigaku diffractometer (Ultima IV). The conditions were slit fixed at 10 mm, 0.5 mmPb monochromatic radiation, 40 mA, and 40 kV. The samples were run at a speed of $30°/\text{min}$ ($20°$–$70°$).

3.2. Statistical Analysis

In environmental science, multivariate analysis has become a more powerful tool than the classical single-variable method because it simplifies data analysis [18]. Multivariate analysis methods, such as principal component analysis (PCA) and factor analysis (FA), have been successfully applied to assess the quality of water and stream sediments and to identify the chemical processes therein [19–22].

To characterize and compare these parameters, SPSS Statistics v22 software (International Business Machines Corporation, Amenk, NY, USA) was used to analyze the chemical properties of the water and stream sediment samples. PCA was applied to a water quality variable analysis [23], and FA quickly simplified the data by extracting eigenvalues and eigenvectors from the correlation coefficient matrix [24]. The Kaiser–Meyer–Olkin (KMO) and Bartlett tests of sphericity have frequently been used to test the appropriateness of FA for the data. In our study, the sphericity (0.6) was greater than 0.5, and the KMO result was less than 0.001, indicating that the data were suitable for FA. In total, eight parameters of pH, EC, HCO_3^-, SO_4^{2-}, Cl, Na, Ca, and Mg were measured in the water samples, while 15 parameters of Cr, Mn, Co, Ni, Cu, Zn, Rb, Sr, Pb, P, Ti, Al_2O_3, CaO, Fe_2O_3, and MgO were measured in the stream sediment samples that were used in the statistical analysis of the data.

4. Results and Discussion

4.1. Hydrochemical Characteristics

The physicochemical and chemical properties of the water samples from the study area are summarized in Tables 1 and 2. Water samples P6 and P12 were collected upstream from the Xiaojiagou and Kongjiagou coal mine drainages, respectively, to represent the two background values. The temperature difference between the groundwater and the stream was approximately 10.0 °C, which could have been affected by the temperature exceeding 22.0 °C during collection. In the dry season, the groundwater and stream samples were slightly alkaline with pH values of 7.1–8.2 and 7.6–8.1, respectively. Compared to the dry season, the pH values of groundwater were slightly acidic to alkaline (6.7–8.2) and the stream samples were alkaline (7.7–8.3) in the wet season. Most stream water samples had EC values higher than those of the groundwater samples in both the dry and wet seasons. Except for P3, which had the highest TDS value, the groundwater seemed to be more pure and contained less dissolved solids. Moreover, the groundwater and stream samples were oxidized, except for two samples (P2 and P4 in the dry season) that had negative Eh values, where more oxygen was found in the stream samples than in the groundwater samples. Furthermore, a Piper diagram [25] was used to analyze the main ions present in the water to highlight the relative concentration of each ion in the water samples, which were divided

into nine areas to show the differences in the geochemical characteristics and groundwater composition types in each area. Most groundwater and stream samples from the dry and wet seasons were dominated by $Ca^{2+} + Mg^{2+} - HCO_3^-$ and $Ca^{2+} + Mg^{2+} - Cl^-$, as shown in the Piper diagram (Figure 4). The coal mine drainage samples (P2 and P3) were dominated by $Ca^{2+} + Mg^{2+} - Cl^- + SO_4^{2-}$, whereas the groundwater sample (P4) was dominated by $Ca^{2+} + Na^+ - HCO_3^-$. Stiff diagrams (Figures S1 and S2) were used to depict the chemical state of groundwater. The high concentration of Ca^{2+} and SO_4^{2-} in P3, P14, and P15 can be explained by the dissolution of the gypsum. The excess Ca^{2+} and HCO_3^- in P6 and P7 may be related to the dissolution of carbonate.

Table 1. Physico-chemical and chemical results of water samples in the study area (dry season).

| Sample | Type | Physico-Chemical Parameters | | | | | Concentration (mg/L) | | | | | | | | |
		T (°C)	pH	Eh (mV)	DO (mg/L)	EC (μS/cm)	TDS	HCO$_3^-$	SO$_4^{2-}$	Cl$^-$	K$^+$	Na$^+$	Ca^{2+}	Mg^{2+}	Si
detection limits		5	0.1	0.1	0.01	10	20	2.5	0.018	0.007	0.02	0.02	0.03	0.02	0.01
P1	gw	16.1	7.1	+46.0	9.2	195.0	138.0	73.2	49.2	1.3	1.8	3.2	27.9	6.0	4.7
P2	gw	17.6	7.9	−10.6	8.7	375.0	268.0	82.2	128.9	1.6	1.8	7.9	44.7	15.2	12.1
P3	gw	16.8	7.9	+130.7	7.8	1010.0	780.0	153.1	477.0	0.8	4.6	5.7	141.2	56.9	6.8
P4	gw	18.2	7.7	−57.9	5.9	435.0	296.0	248.7	39.0	6.2	1.3	71.1	31.9	5.4	7.6
P5	gw	18.1	7.8	+69.1	8.8	294.0	200.0	121.0	63.7	0.9	1.9	4.0	47.1	9.0	4.9
P6	st	19.6	7.9	+120.7	9.8	205.0	150.0	100.8	38.1	0.9	1.5	2.4	41.3	4.9	3.8
P7	gw	22.5	8.2	+111.6	7.0	248.0	162.0	153.1	17.3	0.8	1.4	2.1	47.5	5.0	4.0
P8	gw	18.9	7.9	+104.9	8.9	593.0	428.0	173.3	193.9	1.4	4.0	18.0	85.5	21.2	7.2
P9	st	20.0	8.0	+115.0	8.8	590.0	432.0	181.5	191.7	1.4	4.0	17.0	88.7	21.1	7.2
P10	st	21.9	8.1	+109.7	8.6	583.0	436.0	175.5	202.8	1.5	3.9	17.4	83.7	20.0	7.0
P11	st	25.7	7.7	+111.1	8.5	582.0	414.0	186.7	171.4	1.7	4.2	20.2	85.9	18.8	7.4
P12	st	26.6	7.7	+114.0	8.5	380.0	246.0	177.7	58.9	6.3	2.7	12.3	55.5	10.5	4.2
P13	st	21.8	7.7	+110.3	8.5	425.0	304.0	115.8	135.4	2.0	3.4	14.5	60.7	14.7	6.4
P14	st	20.7	7.7	+113.7	8.5	435.0	306.0	113.5	138.8	2.0	3.4	14.6	59.8	15.0	6.4
P15	st	20.7	7.6	+115.7	8.3	434.0	310.0	119.5	139.6	2.1	3.5	14.9	59.8	15.2	6.0

Eh—relative to field pH electrode; DO—dissolved oxygen; EC—electrical conductivity; TDS—total dissolved solids; gw—groundwater; st—stream.

Table 2. Physico-chemical and chemical results of water samples in the study area (wet season).

| Sample | Type | Physico-Chemical Parameters | | | | | Concentration (mg/L) | | | | | | | | |
		T (°C)	pH	Eh (mV)	DO (mg/L)	EC (μS/cm)	TDS	HCO$_3^-$	SO$_4^{2-}$	Cl$^-$	K$^+$	Na$^+$	Ca^{2+}	Mg^{2+}	Si
detection limits		0.1	0.1	0.1	0.01	10	20	2.5	0.018	0.007	0.02	0.02	0.03	0.02	0.01
P1	gw	16.8	7.7	+128.5	9.0	52.0	35.0	51.9	19.1	1.4	1.6	2.5	16.9	3.5	6.5
P2	gw	17.4	8.2	+35.8	8.6	341.0	222.0	72.3	129.0	1.5	1.8	7.7	44.3	14.5	8.8
P3	gw	16.3	6.7	+208.6	7.8	685.0	445.0	111.0	318.0	0.6	3.7	4.6	98.3	38.8	8.1
P4	gw	17.1	7.8	+146.5	8.9	115.0	74.0	241.0	15.4	6.7	1.1	70.2	19.1	2.7	6.5
P5	gw	16.3	7.7	+35.6	9.0	146.0	94.0	119.0	23.2	0.9	1.4	2.1	37.7	4.6	5.7
P6	st	15.9	8.3	+74.4	9.7	129.0	84.0	115.0	22.1	0.9	1.3	1.9	35.7	4.0	5.0
P7	gw	15.8	8.2	+115.1	9.0	232.0	150.0	167.0	16.5	1.1	1.4	1.8	51.5	5.1	6.4
P8	gw	18.7	8.0	+123.8	8.6	505.0	328.0	185.0	157.0	1.1	3.4	11.8	81.6	19.4	8.2
P9	st	18.8	8.0	+81.6	9.0	469.0	302.0	187.0	144.0	1.2	3.2	10.5	77.9	17.6	7.2
P10	st	19.7	8.2	+99.6	9.1	463.0	300.0	187.0	142.0	1.2	3.1	10.2	76.0	17.2	7.8
P11	st	19.8	7.7	+54.4	8.2	458.0	297.0	189.0	166.0	1.5	3.9	24.4	74.5	17.4	7.1
P12	st	20.7	8.0	+134.3	8.6	382.0	248.0	100.0	128.0	1.4	3.3	14.6	50.2	12.8	6.4
P13	st	20.3	8.1	+107.6	8.6	390.0	254.0	128.0	106.0	3.1	3.3	15.2	53.8	11.8	6.5
P14	st	20.1	8.0	+100.1	8.8	396.0	257.0	120.0	122.0	2.2	3.4	17.0	52.4	12.4	7.0
P15	st	20.0	8.0	+125.0	8.3	311.0	202.0	122.0	120.0	2.3	3.4	17.1	52.2	12.3	6.9

Eh—relative to field pH electrode; DO—dissolved oxygen; EC—electrical conductivity; TDS—total dissolved solids; gw—groundwater; st—stream.

The Gibbs diagram further indicates the origins and influencing factors of groundwater components [26]. As shown in Figure 5, most samples fell within the water–rock interaction zone in both seasons, indicating that rock mineral wreathing was the major factor controlling the hydrochemicals in the study area. In both the dry and wet seasons, the $Na^+/(Na^+ + Ca^{2+})$ ratio of some water samples was >0.6 and beyond the boundary. This result was obtained mainly because the calculated mass concentration of Na^+ contained other undetermined cation components [5]. The high TDS concentration suggests that there were extensively charged species in the aquifer.
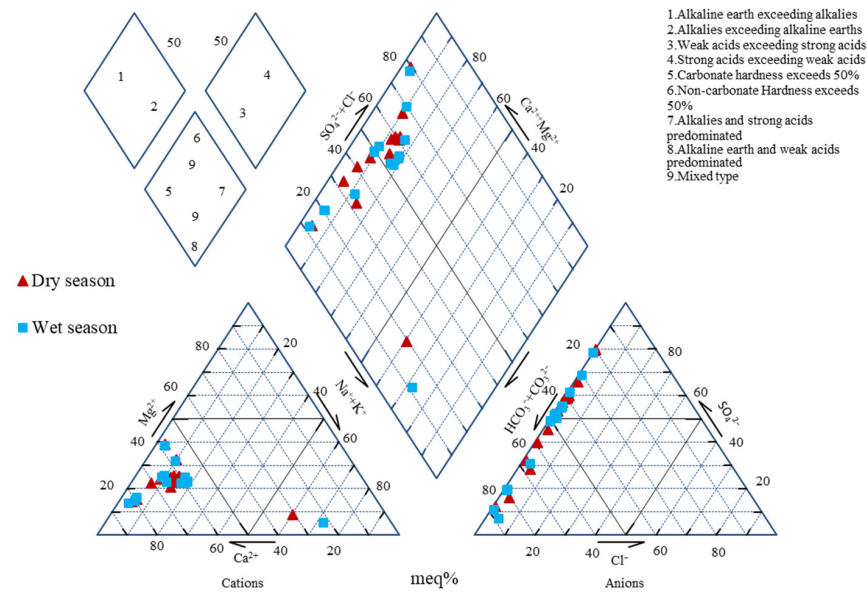
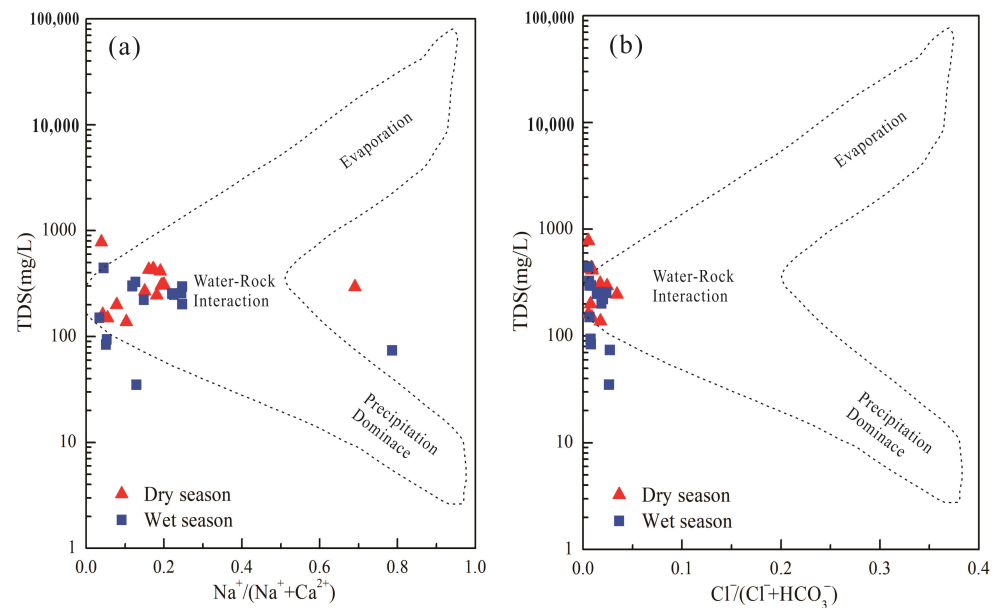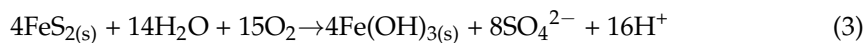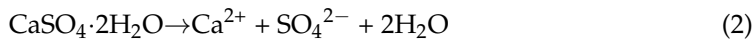**Figure 4.** Piper diagram showing the type of water samples of the study area.
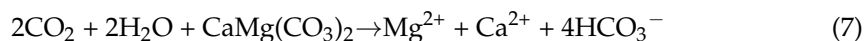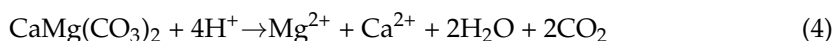

Figure 5. Gibbs diagram explaining the hydrogeochemical processes: (**a**) $Na^+/(Na^++Ca^{2+})$ vs. TDS and (**b**) $Cl^-/(Cl^-+HCO_3^-)$ vs. TDS.

The $\gamma(Ca^{2+})/\gamma(SO_4^{2-})$ ratios of most water samples in Figure 6a are 1:1. This finding can be explained by the complex influences of the dissolution and evaporation processes of gypsum and anhydrite (Equations (1) and (2)). Some water samples showed Ca^{2+}/SO_4^{2-} ratios greater than 1, indicating the addition of Ca by the weathering of Ca-rich minerals, which may involve calcite and dolomite dissolution. The coal mine drainage sample (P3) had Ca^{2+}/SO_4^{2-} ratios of less than 1 in both the dry and wet seasons. This characteristic may have been due to the oxidation of sulfides in the coal seams, such as pyrite (FeS_2), which produced a free acid that neutralized the carbonate minerals in the coal measures [27]. This reaction can be explained by Equation (3).

$$CaSO_4 \rightarrow Ca^{2+} + SO_4^{2-} \tag{1}$$

$$CaSO_4 \cdot 2H_2O \rightarrow Ca^{2+} + SO_4{}^{2-} + 2H_2O \tag{2}$$

$$4FeS_{2(s)} + 14H_2O + 15O_2 \rightarrow 4Fe(OH)_{3(s)} + 8SO_4{}^{2-} + 16H^+ \tag{3}$$

As shown in Figure 6b, most water samples were above the $Mg^{2+} + Ca^{2+}/HCO_3{}^-$ ratio 1:1 line, indicating that excess Ca^{2+} and Mg^{2+} may be related to the dissolution of carbonate [28] (Equation (4)). Carbonate minerals, such as calcite, dolomite, iron dolomite, and siderite, are usually filled in coal fractures as epigenetic minerals [29] and are mainly formed by the reaction of CO and CO_2 produced during coalification with the fluid in coal [30]. Sample P4 had an $Mg^{2+} + Ca^{2+}/HCO_3{}^-$ ratio exceeding 1:2, indicating that more CO_2 entered the groundwater and generated a large amount of $HCO_3{}^-$ during the flow process [5] (Equation (5)). In addition, the concentrations of major ions in the stream water samples were higher than those in the groundwater samples, especially in the cases of $HCO_3{}^-$ and Ca^{2+}. Owing to the enclosure of the environment, the CO_2 released by the neutralization reaction further deepened dissolution [31], which can be explained by Equations (6) and (7).

$$CaMg(CO_3)_2 + 4H^+ \rightarrow Mg^{2+} + Ca^{2+} + 2H_2O + 2CO_2 \tag{4}$$

$$CO_{2(g)} + H_2O \rightarrow H^+ + HCO_3{}^- \tag{5}$$

$$CO_2 + H_2O + CaCO_3 \rightarrow Ca^{2+} + 2HCO_3{}^- \tag{6}$$

$$2CO_2 + 2H_2O + CaMg(CO_3)_2 \rightarrow Mg^{2+} + Ca^{2+} + 4HCO_3{}^- \tag{7}$$

Therefore, $Ca \cdot Mg\text{-}HCO_3$ groundwater was continuously discharged from the pithead, which increased the ionic concentration in the downstream drainage. It should be noted that the concentration of $SO_4{}^{2-}$ in the groundwater sample (P3) was 477.0 mg/L during the dry season, which exceeded the limit value of 250 mg/L in the Chinese drinking water standard; hence, it is not suitable for use as a drinking water source. However, local residents still place water pipes at the pithead to use this water for drinking, which would have a certain impact on their health.
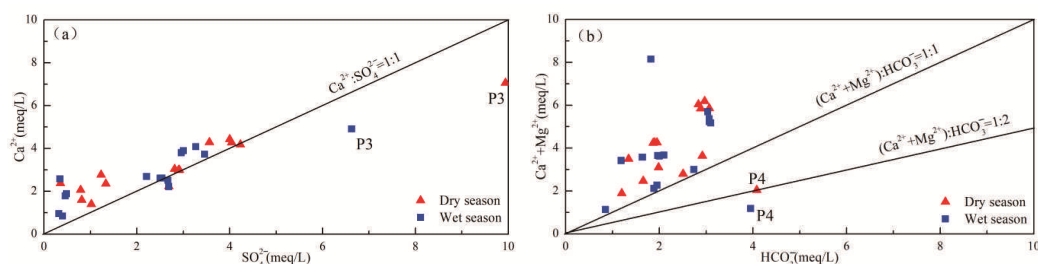

Figure 6. Scatter plots showing the relationships between: (**a**) $SO_4{}^{2-}$ vs. Ca^{2+} and (**b**) $HCO_3{}^-$ vs. $(Ca^{2+} + Mg^{2+})$.

Box plots are used to represent the concentration of the major elements in Figure 7. The median is plotted near the center with log boxes of different parameters, indicating the maximum number of parameters in the normal distribution. The exceptions are the non-normal distributions of $SO_4{}^{2-}$, $HCO_3{}^-$, and Ca^{2+}. The imbalance in $SO_4{}^{2-}$ is mainly due to the large amount of AMD produced by abandoned mines in the oxidation environment, where AMD is discharged into downstream rivers. These results show that in the dry season, the concentrations of SO_4 in groundwater samples P3 and P8 are 477 mg/L and 193.9 mg/L, respectively, and the same phenomenon is observed in the wet season. The collected water samples were mainly from the coal mine drainage at the pithead and river water downstream from the drain. These water samples were collected from hills,

wastelands, alluvial plains, and underground mines in the study area. Land use and land cover patterns can directly affect the water and chemical properties of the study area. Therefore, the variations of these parameters would appear not to be normally distributed, which could be caused by coal mining as well as agricultural and domestic waste [32].
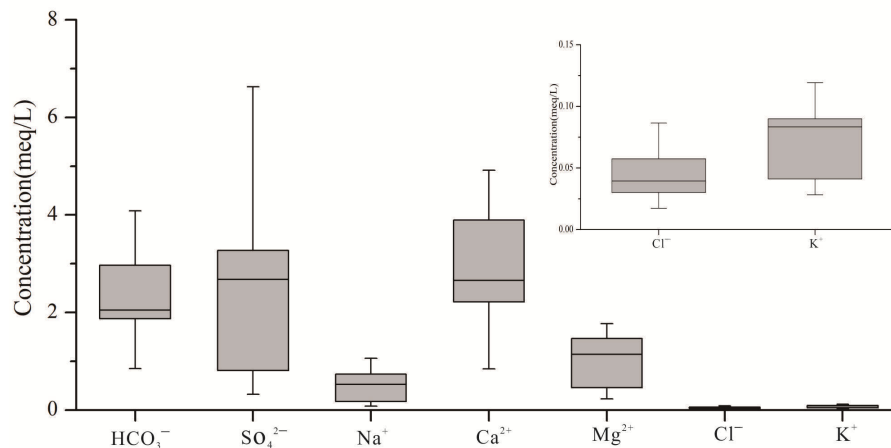

Figure 7. Box plots for the concentration of major elements.

4.2. Trace Elements Concentration of the Water Samples

The concentration of 10 trace elements, including Zn, Fe, Mn, and Al in each water sample, are summarized in Table 3. The water quality properties in the study area, according to the Chinese Standards for Drinking Water Quality (GB 5749-2006) and the WHO [12], are also provided in Table 3. The concentration of heavy metals (Cr, Cu, Zn, As, Cd, Hg, and Pb) in the water samples is significantly below the CNS and WHO guidelines in Table S1; hence, it was not analyzed in this study. Although a comparison between the ion concentration of all trace elements and the above two standards is not included, this can be regarded as a general indication of the state of water quality in the study area. Iron and Mn clearly exceed the Chinese and WHO standards, whereas other trace elements are within suitable limits. The high concentrations of Mn in five water samples (P1, P2, P4, P5, and P8) during the dry season are 353.38 μg/L, 1925.14 μg/L, 132.88 μg/L, 100.86 μg/L, and 108.04 μg/L, respectively. The Mn concentration in the P2 water sample clearly exceeds the standard, reaching 1925.14 μg/L. The concentration of Fe in water samples P1, P2, P5, P7, P10, P13, and P14 also exceeds the standard value in the dry season, where the concentration of Fe in water sample P2 is 8356.48 μg/L, and those of P1 and P5 are 1563.72 μg/L and 1112.56 μg/L, respectively. The concentration of Fe in the stream water samples is approximately 300 μg/L, and the excess content is less than 100 μg/L in the dry season. Only two samples exist with excessive Mn concentration, P2 and P4, whereas there is an excessive concentration of Fe in water samples P2 and P11 in the wet season, where the concentration of Fe in P2 is 12,872.88 μg/L. The oxidation of iron sulfide and aluminosilicate minerals by acidic water is the main reason for the high concentration of Fe and Mn in coal mine drainage [33,34]. Thus, the reason for the high concentration of Fe and Mn in P2 is the existence of considerable amounts of iron and manganese oxides at the pithead when the mine was abandoned.

Excessive Fe and Mn content in drinking water would have adverse effects on the human body; Fe can affect the cardiovascular system, and Mn can affect the central nervous system as well as brain and reproductive functions, causing anorexia, vomiting, and diarrhea [35]. According to the evaluation based on the Chinese standards for ground water quality (GB 14848-2017), groundwater sample P2 was classified as a class V groundwater sample because of the Fe and Mn contents exceeding 2000 μg/L and 1500 μg/L, respectively, which would not be suitable for drinking.

Table 3. Concentration of trace elements of water samples from the study area.

Element (µg/L)	P1	P2	P3	P4	P5	P6	P7	P8	P9	P10	P11	P12	P13	P14	P15	CNS	WHO
Dry season																	
Li	9.09	16.98	117.19	8.49	9.32	3.11	4.01	35.90	27.01	29.31	27.11	6.44	24.66	13.79	22.83		
B	26.29	51.60	162.97	120.31	46.54	27.73	25.39	187.51	161.07	182.30	183.05	53.78	125.28	124.04	120.66		
Al	46.07	17.92	8.22	56.58	68.66	20.95	15.08	70.34	63.47	114.04	126.02	113.19	136.09	176.37	126.89	200.00	200.00
Ti	2.21	0.24	0.57	0.83	1.46	0.66	0.10	0.43	1.10	3.72	1.91	29.94	2.82	3.16	2.43		
Mn	**353.38**	**1925.14**	36.49	**132.88**	**100.86**	5.67	16.74	**108.04**	70.77	54.54	35.03	29.82	11.46	14.99	19.68	100.00	100.00
Fe	**1563.72**	**8356.48**	44.58	260.37	**1112.56**	59.65	**396.19**	284.88	271.80	**366.17**	231.08	164.87	**366.40**	**360.29**	279.87	300.00	300.00
Ni	7.09	5.88	6.12	0.30	0.84	0.33	3.33	4.61	3.87	3.20	2.00	0.71	9.26	9.81	10.35	20.00	70.00
Zn	22.22	14.35	15.65	6.49	11.32	9.34	24.17	11.77	8.52	8.80	8.45	9.01	24.63	26.59	21.99	1000.00	3000.00
Mo	0.45	0.13	0.40	0.42	0.64	0.25	0.34	3.06	3.15	2.77	2.25	0.56	0.71	0.74	0.73		
Ba	57.36	33.35	25.72	158.33	53.70	36.58	46.01	84.46	82.84	85.66	88.20	66.81	45.38	47.36	49.17	700.00	700.00
Wet season																	
Li	3.86	13.71	98.21	1.76	2.07	1.68	2.20	23.86	19.49	19.04	31.22	20.58	15.40	18.71	15.92		
B	20.98	34.87	96.49	71.06	14.20	11.69	11.24	107.76	105.70	92.53	137.63	101.59	90.57	108.89	103.34		
Al	37.79	35.00	26.05	46.11	19.29	22.53	41.57	29.89	47.23	98.53	166.06	30.85	65.29	55.03	71.31	200.00	200.00
Ti	0.45	0.31	0.34	1.83	0.19	0.19	0.44	0.15	0.59	1.38	1.81	0.19	1.46	2.50	1.94		
Mn	57.33	**1883.86**	72.80	**136.58**	21.52	5.30	10.89	15.57	10.28	17.44	69.50	1.70	15.08	14.39	17.46	100.00	100.00
Fe	228.75	**12,872.88**	34.76	203.91	157.45	52.04	73.69	163.86	128.57	221.19	**428.38**	63.66	126.59	103.53	118.08	300.00	300.00
Ni	2.24	6.29	10.84	0.26	0.26	0.34	0.37	2.59	2.13	1.98	3.59	10.98	7.35	7.76	6.51	20.00	70.00
Zn	2.65	6.65	10.13	0.63	0.33	1.30	39.49	1.97	1.67	1.79	21.02	10.53	6.78	6.45	4.89	1000.00	3000.00
Mo	0.23	0.09	0.26	0.46	0.30	0.27	0.27	3.47	2.77	2.43	1.51	0.66	0.77	0.90	0.87		
Ba	42.58	33.44	20.19	167.42	37.27	28.66	48.37	93.69	84.68	85.10	100.74	34.52	44.84	42.66	43.81	700.00	700.00

CNS: China Standard (GB 5749-2006); WHO: World Health Organization [12]. Elements' content exceeding criteria given by legislation are shown in bold characters.

4.3. Variation of Downstream Concentration

The variations in the major ionic concentration from the coal mine drainage to the downstream area are depicted in Figure 8. The drain outlets (source of contamination) of the two coal mines are located at the 0 m position. In both the dry and wet seasons, P6 and P12 were collected upstream, near the drain outlets, and their main ion concentrations (at X = 0) can be used as background values for comparison with downstream water samples. This finding shows that the concentrations of most major ions are higher than the background values. However, the concentration of HCO_3^- in water sample P12 is higher than that of the downstream water sample, indicating the presence of $Ca \cdot Mg\text{-}HCO_3$ in the groundwater upstream from the Kongjiagou coal mine drainage, which is enriched with HCO_3^-. Compared with the background value, the Mn concentration downstream from Kongjiagou shows little change. It can also be observed that the ion concentration is highest at the beginning of the drain and gradually decreases with the downstream distance. However, downstream of the Kongjiagou drain, the concentrations of Mg, SO_4^{2-}, and HCO_3^- did not decrease with distance but rather increased slightly. This may be due to the fact that Kongjiagou was a coal mine and was constantly discharging mine water into the river, resulting in the river water being in a state of ion enrichment for a long period of time. Hence, coal mine drainage from the Xiaojiagou coal mine (P8) led to the enrichment of Ca^{2+}, Mg^{2+}, SO_4^{2-}, HCO_3^-, Fe, and Mn. The high concentration of these major ions indicate the impact of the coal mine drainage on the water quality of the aquifer.
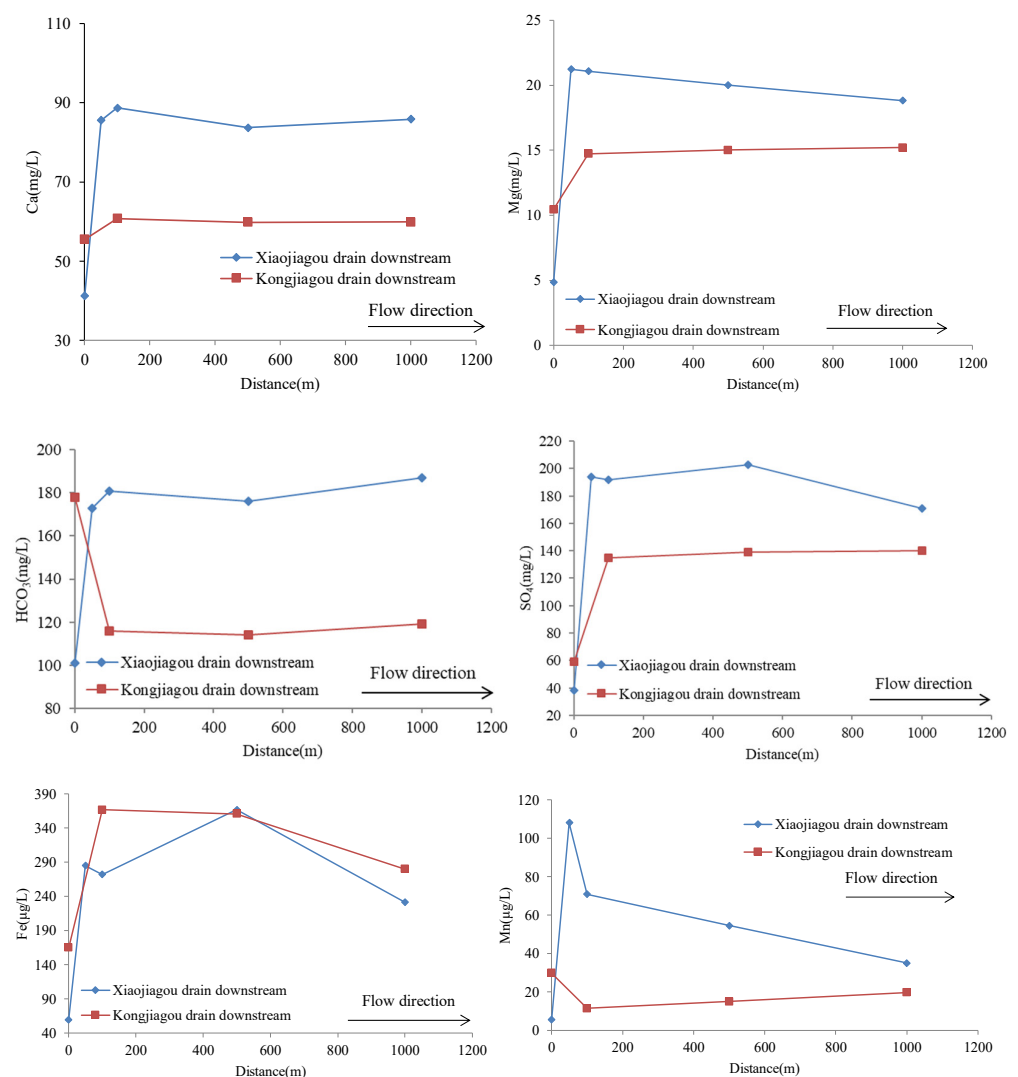

Figure 8. Variation between the concentration of major ions and the distance downstream.

4.4. Statistical Analysis of the Water Samples Dataset

Eight variables across 15 samples were used to analyze the correlations. The correlation matrix results, including the physicochemical parameters, are summarized in Table 4, which shows that the pH is negatively correlated with Ca^{2+}. The EC is positively correlated with HCO_3^-, SO_4^{2-}, Mg^{2+}, and Ca^{2+}; HCO_3^- is positively correlated with Cl^- and Na^+; and SO_4^{2-} is positively correlated with Ca^{2+} and Mg^{2+}. In addition, Cl^- is positively correlated with Na^+, and Ca^{2+} is positively correlated with Mg^{2+}. Moreover, strong positive correlations are observed between EC and SO_4^{2-}, EC and Ca^{2+}, EC and Mg^{2+}, HCO_3^- and Na^+, SO_4^{2-} and Ca^{2+}, SO_4^{2-} and Mg^{2+}, Cl^- and Na^+, and Ca^{2+} and Mg^{2+}. Some moderate and positive correlations are also observed in between HCO_3^- and Cl^-.

Table 4. Correlation matrix of physico-chemical parameters in waters.

	pH	EC	HCO_3^-	SO_4^{2-}	Cl^-	Na^+	Ca^{2+}	Mg^{2+}
pH	1.00							
EC	−0.40	1.00						
HCO_3^-	−0.14	0.42	1.00					
SO_4^{2-}	−0.36	0.95 **	0.12	1.00				
Cl^-	0.06	−0.08	0.55 *	−0.30	1.00			
Na^+	0.22	0.14	0.74 **	−0.12	0.69 **	1.00		
Ca^{2+}	−0.49	0.94 **	0.28	0.94 **	−0.29	−0.14	1.00	
Mg^{2+}	−0.35	0.94 **	0.12	0.99 **	−0.27	−0.14	0.94 **	1.00

* Correlation is significant at the 0.05 level. ** Correlation is significant at the 0.01 level.

F1 is positively correlated with the EC, SO_4^{2-}, Ca^{2+}, and Mg^{2+} and negatively correlated with the pH (Table 5), explaining 52% of the data variance. Moreover, F1, which is correlated with SO_4^{2-}, results in a higher overall concentration, which could be related to sulfide minerals [36], whereas the positive correlations between F1 and both Ca^{2+} and Mg^{2+} also indicate that a large amount of carbonate minerals is dissolved during the process of atmospheric precipitation moving underground through the surface. Simultaneously, F1 displays a negative correlation with most of the dissolved minerals and pH. When the concentration of dissolved minerals increases, the pH decreases. These observations are primarily found in the context of AMD [37]. Therefore, F1 can be considered an indicator of AMD. Furthermore, the F2 factor is positively correlated with HCO_3^-, Cl^-, and Na^+ (Table 5), which explains 29% of the data variance, and is correlated with the ions that characterize the carbonate minerals. The Na^+ and Cl^- ions were mainly produced by precipitation, human activities, and the dissolution of silicates [32]. In the studied case, a strong positive correlation was observed between Na^+ and Cl^-, indicating a strong degree of dissolution evaporation in this area. Consequently, F2 can be considered as an indicator of halite dissolution. Hence, F1 can represent the high concentrations of SO_4^{2-}, Ca^{2+}, Mg^{2+}, and low pH in the abandoned coal mine drainage, and F2 can represent the relationships between the drainage and the HCO_3^-, Na^+, and Cl^- concentrations in downstream rivers [38].

4.5. Geochemistry of Stream Sediments

The concentration of metals and metalloids in the seven stream sediment samples near the mine drain were measured (Table 6) and are displayed as box and whisker plots of the concentration of each element (Figure 9). The concentration of Al (%), Ca (%), Mg (%), Fe (%), and Mn (ppm) in the two streams downstream of the drain are significantly different. The concentration of Ca in the stream sediments downstream of the Xiaojiagou drain is on average–3–4 times higher than that in Kongjiagou, whereas the concentration of Mg in the downstream sediments of the Kongjiagou drain is higher than that in Xiaojiagou. These findings demonstrate that large amounts of carbonate minerals are present in the stream sediments. These minerals are produced by the leaching of groundwater into a karst aquifer, which is subsequently discharged. It is worth noting that the concentrations of Fe,

Mn, Cr, and Zn downstream from the Kongjiagou drain are evidently higher than those in Xiaojiagou, and the concentration of Mn is 5–6 times higher. This result clearly indicates that the Xiaojiagou coal mine is closed, whereas the Kongjiagou coal mine remains active. With mining activities, a large amount of metal minerals is discharged and deposited downstream of the coal mine drainage, affecting water and soil quality. In addition, the concentrations of Fe and Mn oxides in the anoxic zone are relatively low, whereas the concentrations of dissolved Fe and Mn in the interstitial water increase accordingly [39].

Table 5. Factor loadings and communalities of water parameters dataset.

	F1	**F2**	**Communalities**
pH	**−0.51**	0.07	0.26
EC	**0.97**	0.21	0.99
HCO_3^-	0.27	**0.88**	0.84
SO_4^{2-}	**0.97**	−0.09	0.95
Ca^{2+}	**0.99**	−0.03	0.75
Mg^{2+}	**0.97**	−0.08	0.87
Cl^-	−0.25	**0.83**	0.97
Na^+	−0.08	**0.93**	0.94
Eigenvalues	4.19	2.38	
% of variance explained	52.41	29.81	
Cumulative % of variance	52.41	82.21	

Loading values for the PC axis higher than +0.5 and lower than −0.5 are given in bold.

Table 6. Concentrations of metals and metalloids of stream sediments near the mine drain. All values are in ppm, except for Al_2O_3, CaO, Fe_2O_3, and MgO (%).

	S1	**S2**	**S3**	**S4**	**S5**	**S6**	**S7**	**NSB**
Cr	33.0	44.1	33.7	62.7	51.1	56.8	69.9	62
Mn	388.2	615.9	355.0	2197.1	2402.7	2111.5	1428.9	640
Co	14.1	14.8	21.3	16.5	17.2	18.8	19.6	12
Ni	18.4	21.6	15.3	28.8	26.5	44.9	43.8	25
Cu	22.4	23.1	85.3	27.4	24.4	24.4	30.9	21
Zn	49.9	56.2	48.0	81.6	74.6	91.4	102.0	70
Rb	51.4	65.6	65.4	95.7	80.7	86.1	109.0	/
Sr	344.8	285.3	127.5	136.2	163.8	172.6	157.1	83
Pb	19.5	17.7	19.4	23.8	21.9	22.8	27.7	25
P	442.6	480.5	285.7	548.0	489.7	447.8	603.1	521
Ti	1825.0	2157.0	2446.0	3671.0	3349.0	3601.0	4328.0	4222
Al_2O_3	7.9	8.3	7.7	13.9	11.6	13.3	15.3	13.1
CaO	19.9	16.2	4.8	4.5	5.7	5.2	3.5	0.8
Fe_2O_3	2.4	3.8	2.7	6.4	5.1	5.8	6.7	4.4
MgO	0.7	0.8	0.6	1.4	1.2	1.3	1.4	1.1

NSB: China stream sediments background value [40].

Compared with the average background values in a low mountainous or hilly area [40], the concentrations of Pb, P, and Ti in the seven samples were similar to the background values, whereas the concentrations of Cr, Mn, Ni, Zn, Al, Fe, and Mg in the stream sediments downstream from the Kongjiagou drain were higher than the background values, and the concentrations of Fe and Mn ions were 3–4 times higher than the background values. The samples (S1–S3) taken downstream of the Xongjiagou drain were all below the background values. Thus, with continuous mining activities, large amounts of Fe and Mn oxides were discharged into the downstream river along with coal mine drainage, resulting in the enrichment of Fe and Mn in the downstream sediments. Hence, the closure of coal mines is beneficial for the recovery of the local environment and has a positive ecological effect.
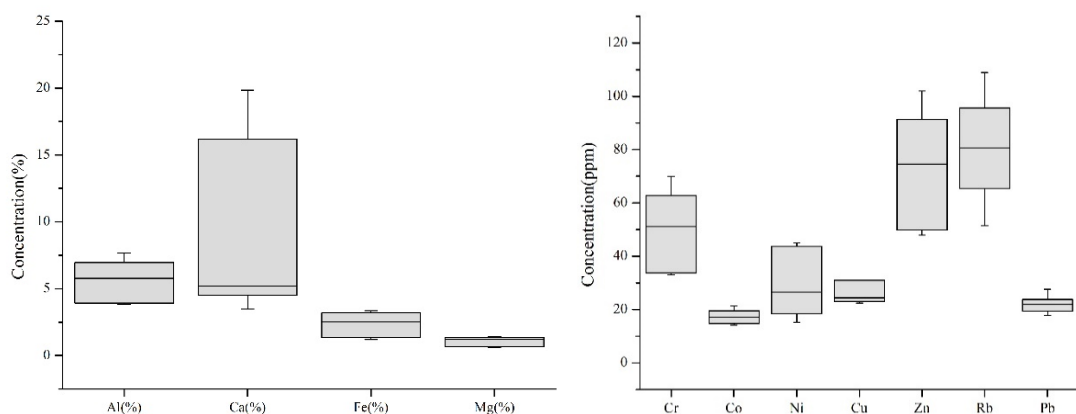
Figure 9. Box plots for the concentration of metals and metalloids.

Furthermore, the concentrations of Co, Cu, Sr, and Ca in all the samples exceeded the background values. The concentration of Cu in sample S3 was as high as 85.3 ppm, which may have been caused by local human activities (domestic waste and fertilization) [32], and the concentrations of Ca in samples S1 and S2 downstream from the Xongjiagou drain were much higher than those in the other samples, indicating that carbonate dissolution took place in the Xiaojiagou coal mine. These phenomena can be explained by the dissolution and precipitation of minerals (calcite and dolomite) during stream sedimentation and mine drainage [5]. Hence, according to the standard environmental quality evaluation for soil analysis (GB 15618-1995), all seven stream sediment samples had good-quality soil, reflecting the secondary standard of environmental quality. This type of soil is suitable for planting and animal husbandry, and the soil quality does not cause harm or pollution to the environment.

4.6. Statistical Analysis of the Stream Sediments Samples Dataset

The correlation matrix of the stream sediment samples (Table 7) highlights that Cr has strong positive correlations with Zn, Rb, Pb, Ti, Al, Fe, and Mg and moderately positive correlations with Ni and P. This may be because some chromium minerals, such as picotite (Fe $(Cr, Al)_2O_4$), enter the stream with groundwater during mining [41]. Moreover, Mn has a strong positive correlation with Mg and moderately positive correlations with Ti, Al, and Fe. Co has a strong negative correlation with Sb and moderately negative correlations with Sr and Ca. High positive loadings of these elements indicate a strong connection with mining. Coal mine drainage causes minerals rich in these elements to enter into the river, leading to an increase in these elements in stream sediments, which subsequently affects the stream water [42]. Furthermore, Ni has strong positive correlations with Zn and Al and moderately positive correlations with Rb, Pb, Ti, Fe, and Mg. In addition, Zn exhibits strong positive correlations with Rb, Pb, Ti, Al, Fe, and Mg. The relationships between Ni and Zn indicate the effect of local human activities (domestic waste and fertilization) and lithology (weathering of parent rocks) [32]. Al has strong positive correlations with Fe and Mg, whereas Fe has a strong positive correlation with Mg. Hence, the stream sediment correlations reflect the adsorption capacities of Fe, Mn, and Al oxides in metals and metalloids within the surface environment [43]. This finding also highlights the influence of coal mine drainage, because the concentrations of Fe, Zn, Mn, Cr, Al, and Mg in the stream sediments directly obtained from the coal mine drainage are the highest (Table 6).

Table 7. Correlation matrix in stream sediments from the study area.

	Cr	Mn	Co	Ni	Cu	Zn	Rb	Sr	Pb	P	Ti	Al$_2$O$_3$	CaO	Fe$_2$O$_3$	MgO
Cr	1.00														
Mn	0.73	1.00													
Co	0.22	0.10	1.00												
Ni	0.85 *	0.63	0.30	1.00											
Cu	−0.41	−0.45	0.72	−0.42	1.00										
Zn	0.96 **	0.74	0.31	0.95 **	−0.40	1.00									
Rb	0.97 **	0.69	0.43	0.81 *	−0.19	0.93 **	1.00								
Sr	−0.52	−0.55	−0.81 *	−0.37	−0.45	−0.51	−0.69	1.00							
Pb	0.89 **	0.59	0.40	0.81 *	−0.21	0.91 **	0.92 **	−0.55	1.00						
P	0.82 *	0.53	−0.31	0.61	−0.75	0.73	0.70	−0.01	0.69	1.00					
Ti	0.94 **	0.76 *	0.48	0.84 *	−0.19	0.95 **	0.98 **	−0.72	0.93 **	0.63	1.00				
Al$_2$O$_3$	0.98 **	0.78 *	0.29	0.88 **	−0.38	0.98 **	0.96 **	−0.56	0.94 **	0.75	0.97 **	1.00			
CaO	−0.63	−0.62	−0.81 *	−0.53	−0.34	−0.65	−0.78 *	0.98 **	−0.13	−0.83 *	−0.68		1.00		
Fe$_2$O$_3$	0.99 **	0.81 *	0.24	0.85 *	−0.41	0.96 **	0.96 **	−0.58	0.86 *	0.77 *	0.95 **	0.98 **	−0.68	1.00	
MgO	0.96 **	0.88 **	0.18	0.84 *	−0.48	0.95 **	0.92 **	−0.54	0.85 *	0.78 *	0.94 **	0.97 **	−0.65	0.98 **	1.00

* Correlation is significant at the 0.05 level. ** Correlation is significant at the 0.01 level.

4.7. Correlations with Coal Mine Drainage

Based on the data analysis results summarized in Tables 1, 2 and 6, the closure of the Xiaojiagou coal mine caused groundwater to remain in the abandoned mine channel longer than in the Kongjiagou coal mine. In addition, the groundwater samples have a weakly acidic environment, which is conducive to the dissolution of carbonate minerals. Therefore, the concentrations of Ca^{2+} and Mg^{2+} in the water samples downstream from Xiaojiagou (P8–P11) are significantly higher than those in downstream water samples P12–P15. This phenomenon directly increases the Ca^{2+} content in the downstream sediments to far higher than the background value, and the concentrations of Ca in Xiaojiagou are higher than those in Kongjiagou. During the mining process, many minerals containing Fe and Mn are dissolved or suspended in the groundwater along with the discharged mine water inflow, forming downstream stream sediments [44]. Consequently, the Fe and Mn contents in the stream sediments (S4–S7) in the lower reaches of Kongjiagou are much higher than the background values.

An XRD analysis was performed on two stream sediment samples (S1 and S4). Mineral phases such as quartz and cuprite are observed in both samples (Figure 10). Magnetite and delafossite, which are characteristics of weathered mining waste, indicate the possible presence of various mineral phases of environmental interest [45]. Muscovite and pyrite are evident in each sample, indicating that the coal mine drainage transported these minerals from the strata into the stream. Calcite is the major mineral phase in S1 and belongs to the waste-rock deposit of the Xiaojiagou coal mine. In addition, a large amount of quartz in the Xujiahe Triassic Formation entered the river with the coal mine drainage (Figure 11).

Generally, the concentration of metals and metalloids in the stream sediments were affected by the coal mine drainage and were generally enriched in Cr, Mn, Zn, Sr, Co, Ni, Cu, Al, Ca, Fe, and Mg, and the concentrations of Mn, Ca, and Fe were significantly increased. These findings demonstrate that strong positive correlations exist between the concentrations of trace elements in coal mine drainage and stream sediments.
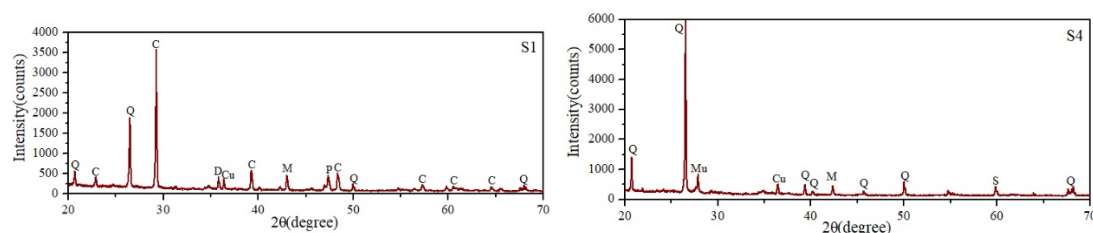

Figure 10. The X-ray diffraction patterns of stream sediment samples. C—calcite; Cu—cuprite; D—delafossite; M—magnetite; Mu—muscovite; P—pyrite; Q—quartz; S—siderophyllite.
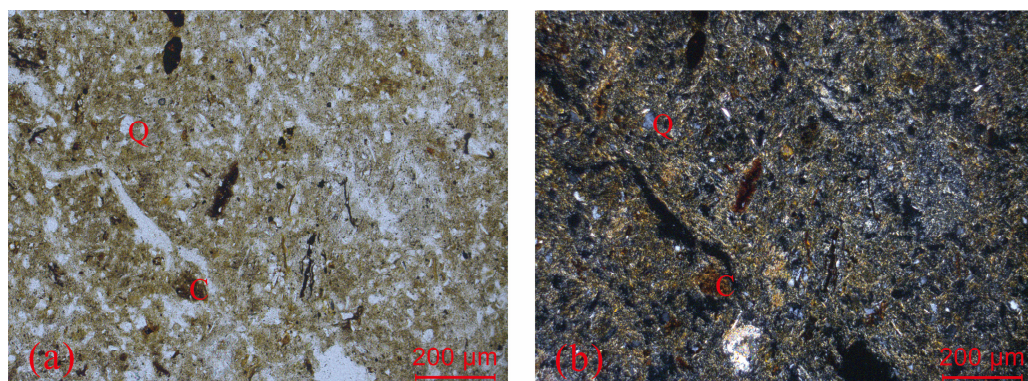
Figure 11. Surface morphology of the stream sediment (S1) in plane polarized light (**a**) and perpendicular polarized light (**b**) under microscope. Q—quartz; C—calcite.

5. Conclusions

The pH of the groundwater samples from the five abandoned mines in the study area ranged from 6.7 to 8.2. With a large amount of coal mine drainage being discharged into the river, the pH of the downstream stream samples of the two drains was weakly acidic. Most of the groundwater and stream samples in the dry and wet seasons are dominated by Ca·Mg-HCO_3 and Ca·Mg-Cl, respectively. SO_4^{2-} originates from gypsum dissolution and pyrite oxidation, and Ca^{2+} and Mg^{2+} may be related to the dissolution of carbonate.

With respect to the Chinese standard and WHO guidelines, the exceptions are the Mn and Fe concentrations, especially in the groundwater samples, which exceed the standard limits for drinking water in China of 100 μg/L and 300 μg/L, with values of 1925.14 μg/L and 12,872.88 μg/L, respectively. In addition, PCA highlighted the SO_4^{2-}, Ca^{2+}, Mg^{2+}, and low pH group as well as the HCO_3^-, Na^+, and Cl^- group, which likely reflect the effects of AMD and human activities and the evaporation occurring in low mountains and hills, respectively.

The average concentrations of Mn and Fe in the downstream Kongjiagou drain sediment samples were 2035.1 ppm and 6%, respectively, which were higher than the Mn and Fe concentrations in Xiaojiagou at 453.1 ppm and 2.9%, respectively. Both the Mn and Fe concentrations were higher than the background values (640 ppm and 4.4%), whereas other elements of samples (S1–S3) from the downstream Xongjiagou drain were below the background values. In summary, long-term monitoring and management of mining activities are required to ensure a safe domestic water supply while maintaining economic development.

Author Contributions: Conception and design of sampling, D.D.; investigation, D.D., B.R., and H.Y.; chemical analysis, D.D. and B.R.; statistical analysis and modeling, D.D.; writing—original draft preparation, D.D. and Y.W.; writing—review and editing, D.D. and Y.W. All authors have read and agreed to the published version of the manuscript.

Data Availability Statement: Not applicable.

Conflicts of Interest: The authors declare no conflict of interest.

References

1.　Du, P.P. *Research on Geologic Environment Effects Induced by Coal Mining in Ecological Weakness Area and Assessment Techniques: A Case Study Taking Yushenfu Mining District in Northern Shanxi Province*; China University of Mining and Technology: Xuzhou, China, 2011.

2.　Alexakis, D.; Gamvroula, D. Arsenic, Chromium, and Other Potentially Toxic Elements in the Rocks and Sediments of Oropos-Kalamos Basin, Attica, Greece. *Appl. Environ. Soil Sci.* **2014**, *2014*, 718534. [CrossRef]

3.　Yoriya, S.; Tepsri, P. Investigation of Metal and Trace Elements of Cenospheres from Lignite High-Calcium Fly Ash (Thailand). *Water* **2021**, *13*, 2935. [CrossRef]

4.　Koukouzas, N.; Ketikidis, C.; Itskos, G. Heavy Metal Characterization of CFB-Derived Coal Fly Ash. *Fuel Process. Technol.* **2011**, *92*, 441–446. [CrossRef]

5.　Heng, Y.; Yong, W.; Lili, J.; Meng, C.; Nisong, P.; Yong, L.; Li, L. Hydrogeochemical vertical zonation and evolution model of the Kongjiagou coalmine in Sichuan, China. *Water Supply* **2022**, *22*, 6111–6129. [CrossRef]

6.　Zhang, Q.X.; Zhou, J.W.; Lin, S.H.; Wei, D.; Zhang, L.; Yuan, L. Characteristics and causes of groundwater pollution after Hongshan-Zhaili mine closure in Zibo. *Saf. Environ. Eng.* **2015**, *22*, 23–28.

7.　Jackson, L.M.; Parbhakar-Fox, A. Mineralogical and geochemical characterization of the Old Tailings Dam, Australia: Evaluating the effectiveness of a water cover for long-term AMD control. *Appl. Geochem.* **2016**, *68*, 64–78. [CrossRef]

8.　Sahoo, S.; Khaoash, S. Impact assessment of coal mining on groundwater chemistry and its quality from Brajrajnagar coal mining area using indexing models. *J. Geochem. Explor.* **2020**, *215*, 106559. [CrossRef]

9.　Zhou, J.; Hu, W.; Zhang, Z. Analysis on rule of groundwater movement and model establishment of current numerical simulation in abandoned mines. *J. China Coal Soc.* **2006**, *31*, 74–77.

10.　Wu, Q.; Li, S. Positive and negative environmental effects of closed mines and its countermeasures. *J. China Coal Soc.* **2018**, *43*, 21–32.

11.　Doulati Ardejani, F.; Jodeiri Shokri, B.; Bagheri, M.; Soleimani, E. Investigation of pyrite oxidation and acid mine drainage characterization associated with Razi active coal mine and coal washing waste dumps in the Azad shahr–Ramian region, northeast Iran. *Environ. Earth Sci.* **2010**, *61*, 1547–1560. [CrossRef]

12.　WHO (World Health Organization). *Guidelines for Drinking-Water Quality*, 4th ed.; WHO: Geneva, Switzerland, 2011.

13.　Jiang, L. The Sedimentary Environment and Coal Accumulating Pattern of Jingang Coalfield in Dazhou. Master's Thesis, Chengdu University of Technology, Chengdu, China, 2016.

14.　Li, Y. Sequence-Palaeogeography and Coal Accumulation of the Late Triassic Xujiahe Formation in the Sichuan Basin. Ph.D. Thesis, China University of Mining and Technology, Beijing, China, 2014.

15.　Jiang, Q. Impact and assessment of Zhenfoshan coal mining of Dazhou on water environment. *Acta Miner. Sin.* **2009**, *29* (Suppl. S1), 398–399.

16.　Hu, W.; Zhou, J.; Yan, L. Study on environment and safety disasters from abandoned coal mines. *J. Xi'an Univ. Sci. Technol.* **2010**, *30*, 436–440.

17.　Li, M.; Wu, H. Coal seam physical property and coal quality characteristics of Jingang coal mine in Dazhou city, Sichuan province. *Mod. Min.* **2018**, *34*, 41–45.

18.　Hou, D.Y.; O'Connor, D.; Nathanail, P.; Li, T.; Ma, Y. Integrated GIS and multivariate statistical analysis for regional scale assessment of heavy metal soil contamination: A critical review. *Environ. Pollut.* **2017**, *231 Pt 1*, 1188–1200. [CrossRef]

19.　Qin, W.J.; Han, D.M.; Song, X.F.; Engesgaard, P. Effects of an abandoned Pb-Zn mine on a karstic groundwater reservoir. *J. Geochem. Explor.* **2019**, *200*, 221–233. [CrossRef]

20.　Narváez, J.; Richter, P.; Toral, M. Preliminary physical chemical characterization of river waters and sediments affected by copper mining activity in Central Chile: Application of multivariate analysis. *J. Chil. Chem. Soc.* **2007**, *52*, 1261–1265. [CrossRef]

21.　Mostert, M.M.; Ayoko, G.A.; Kokot, S. Application of chemometrics to analysis of soil pollutants. *TrAC Trends Anal. Chem.* **2010**, *29*, 430–445. [CrossRef]

22.　Lu, Y.; Tang, C.; Chen, J.; Yao, H. Assessment of major ions and heavy metals in groundwater: A case study from Guangzhou and Zhuhai of the Pearl River Delta, China. *Front. Earth Sci.* **2016**, *10*, 340–351. [CrossRef]

23.　El Amari, K.; Valera, P.; Hibti, M.; Pretti, S.; Marcello, A.; Essarraj, S. Impact of mine tailings on surrounding soils and ground water: Case of Kettara old mine, Morocco. *J. Afr. Earth Sci.* **2014**, *100*, 437–449. [CrossRef]

24.　Davis, J.C.; Sampson, R.J. *Statistics and Data Analysis in Geology*; John Wiley & Sons, Inc.: Hoboken, NJ, USA, 1986; pp. 166–171.

25.　Piper, A.M. A graphical procedure in the chemical interpretation of groundwater analysis. *Trans. Am. Geophys. Union.* **1944**, *25*, 914–923. [CrossRef]

26.　Luan, F.; Zhou, J.; Jia, R.; Lu, C.; Bai, M.; Liang, H. Hydrochemical characteristics and formation mechanism of groundwater in plain areas of Barkol-YiwuBasin, Xinjiang. *Environ. Chem.* **2017**, *36*, 380–389. (In Chinese)

27.　Li, T. Study on Groundwater Pollution Risk Assessment of Abandoned Coal Mine. Ph.D. Thesis, China University of Mining and Technology, Xuzhou, China, 2014.

28.　Lghoul, M.; Maqsoud, A.; Hakkou, R.; Kchikach, A. Hydrogeochemical behavior around the abandoned Kettara mine site, Morocco. *J. Geochem. Explor.* **2014**, *144*, 456–467. [CrossRef]

29.　Ward, C.R. Analysis and significance of mineral matter in coal seams. *Int. J. Coal Geol.* **2002**, *50*, 135–168. [CrossRef]

30. Zhang, N.; Xu, Y.; Ning, S.; Zhao, Y. Mineralogical Characteristics in the No. 6 Coal Seam from the Xiaohuangshan coal mine of Fukang Mining Area, Junggar Coal field. *Coal Sci. Technol.* **2020**, *49*, 9.

31. Zhang, B.H. Study on Ecological Environmental Effect of Coal Mine Closure: A Case Study of Zaozhuang Coal Mining Area. Ph.D. Thesis, Shandong Normal University, Jinan, China, 2016.

32. Deng, D.; Wu, Y.; Sun, Y.; Ren, B.; Song, L. Pollution Characteristics and Spatial Distribution of Heavy Metals in Coal-Bearing Sandstone Soil: A Case Study of Coal Mine Area in Southwest China. *Int. J. Environ. Res. Public Health* **2022**, *19*, 6493. [CrossRef]

33. Cravotta, C.A., III. *Effects of Abandoned Coal-Mine Drainage on Streamflow and Water Quality in the Mahanoy Creek Basin, Schuylkill, Columbia, and Northumberland Counties, Pennsylvania, 2001*; Scientific Investigations Report 2004-5291; U.S. Geological Survey: Reston, VA, USA, 2005.

34. Cravotta, C.A., III. Dissolved metals and associated constituents in abandoned coal-mine discharges, Pennsylvania, USA. Part 2: Geochemical controls on constituent concentrations. *Appl. Geochem.* **2008**, *23*, 203–226. [CrossRef]

35. Peng, Z.J. Treatment of Excessive Iron and Manganese in Groundwater. *Guangdong Chem. Ind.* **2019**, *46*, 130–131.

36. Gamvroula, D.; Alexakis, D.; Stamatis, G. Diagnosis of groundwater quality and assessment of contamination sources in the Megara basin (Attica, Greece). *Arab. J. Geosci.* **2013**, *6*, 2367–2381. [CrossRef]

37. Pope, J.; Newman, N.; Craw, D.; Trumm, D.; Rait, R. Factors that influence coal mine drainage chemistry West Coast, South Island, New Zealand. *N. Z. J. Geol. Geophys.* **2010**, *53*, 115–128. [CrossRef]

38. Chen, M.; Wu, Y.; Gao, D.; Chang, M. Identification of coal mine water-bursting source using multivariate statistical analysis and tracing test. *Arab. J. Geosci.* **2017**, *10*, 28. [CrossRef]

39. Tarutis, W.J., Jr.; Unz, R.F.; Brooks, R.P. Behavior of sedimentary Fe and Mn in a natural wetland receiving acidic mine drainage, Pennsylvania, U.S.A. *Appl. Geochem.* **1992**, *7*, 77–85. [CrossRef]

40. Shi, C.Y.; Liang, M.; Feng, B. Average background values of 39 chemical elements in stream sediments of China. *Earth Sci.* **2016**, *41*, 234–251.

41. Zhao, Y.; Kumul, C.; Wang, T.; Mosusu, N.; Yao, Z.; Zhu, Y.; Zhang, B.; Wang, X. National-Scale Geochemical Baseline and Anomalies of Chromium in Papua New Guinea. *Minerals* **2023**, *13*, 205. [CrossRef]

42. Doufexi, M.; Gamvroula, D.E.; Alexakis, D.E. Elements' Content in Stream Sediment and Wildfire Ash of Suburban Areas in West Attica (Greece). *Water* **2022**, *14*, 310. [CrossRef]

43. Neiva, A.M.R.; Carvalho, P.C.S.; Antunes, I.M.H.R.; Silva, M.M.V.G.; Santos, A.C.T.; Cabral Pinto, M.M.S.; Cunha, P.P. Contaminated water, stream sediments and soils close to the abandoned Pinhal do Souto uranium mine, Central Portugal. *J. Geochem. Explor.* **2014**, *136*, 102–117. [CrossRef]

44. Neiva, A.M.R.; Carvalho, P.C.S.; Antunes, I.M.H.R.; Albuquerque, M.T.D.; Santos, A.C.S.; Cunha, P.P.; Henriques, S.B.A. Assessment of metal and metalloid contamination in the waters and stream sediments around the abandoned uranium mine area from Mortorios, central Portugal. *J. Geochem. Explor.* **2019**, *202*, 35–48. [CrossRef]

45. Rodríguez-Hernández, A.; Lázaro, I.; Razo, I.; Briones-Gallardo, R. Geochemical and mineralogical characterization of stream sediments impacted by mine wastes containing arsenic, cadmium and lead in North-Central Mexico. *J. Geochem. Explor.* **2021**, *221*, 106707. [CrossRef]